EnvironmentAsia
The international journal by the Thai Society of Higher Education Institutes on Environment

EnvironmentAsia 17(1) 2024 148-160
DOI 10.14456/ea.2024.13
ISSN 1906-1714; ONLINE ISSN: 2586-8861

Spatial Association between Environmental Factors and Melioidosis in Thailand

Suwattana Onprasonk[1], Wongsa Laohasiriwong[1*], and Nattapong Puttanapong[2]

[1] *Faculty of Public Health, Khon Kaen University, Khon Kaen, Thailand*
[2] *Faculty of Economics, Thammasat University, Bangkok, Thailand*

*Corresponding author: wongsa@kku.ac.th
Received: August 12, 2023; Revised: September 9, 2023; Accepted: September 24, 2023

Abstract

Melioidosis, dominant in Southeast Asia and northern Australia, is transmitted to humans and animals upon contact with contaminated soil or water in endemic regions. This research evaluated the correlation between environmental factors and melioidosis incidence in Thailand using data from the National Notifiable Disease Surveillance System (Report 506), managed by Thailand's Ministry of Public Health. Satellite-derived environmental data from 2006 - 2020 was sourced from Google Earth Engine. When aggregated at the provincial level and analyzed using bivariate Local Indicators of Spatial Association (LISA), all environmental factors showed a significant relationship with melioidosis incidence ($p < 0.05$), predominantly in the Northeast region. Both fixed- and random-effect regression models revealed similar findings: nearly all satellite-derived environmental factors, except for precipitation in the fixed-effect model ($p = 0.096$), had associations with melioidosis incidence at $p < 0.001$. Specifically, the indicators of vegetation density, night-time land surface temperature, cropland, and precipitation demonstrated positive regression coefficients, while indices representing drought, water bodies, daytime land surface temperature, and urban areas exhibited negative ones. This suggests a connection between optimal climate conditions, agriculture, and melioidosis occurrence. Such satellite data holds potential for informing future prevention measures.

Keywords: Remote sensing; Satellite; Melioidosis; Spatial analysis; Thailand

1. Introduction

Melioidosis, often termed "soil fever," is a disease resulting from the Gram-negative bacterium *Burkholderia pseudomallei*. Transmission to humans and animals primarily occurs through exposure to contaminated soil or water. Notably, this bacterium has an impressive resilience to various conditions, including acidic environments. Within soil, it's predominantly found between depths of 30 - 60 cm, with its presence notably increasing during rainy seasons (Sujuritphong *et al.,* 2014; Wuthiekanun *et al.,* 1995). Those frequently in contact with soil and water, such as farmers and fishermen, face a heightened risk, with incidence peaks in the rainy season due to increased exposure (Kaestli *et al.,* 2016; Currie *et al.,* 2004; Currie *et al.,* 2010).

Melioidosis is epidemic worldwide and endemic in some areas (Chowdhury *et al.,* 2022). Its presence is noted in tropical countries including Thailand, Singapore, Vietnam, China, Taiwan, Laos, Cambodia, Malaysia, Brunei, Northern Australia (White *et al.,* 2003), the southern part of America (Rolim *et al.,* 2005), India (Mukhopadhyay *et al.,* 2018), and Africa (Steinmetz *et al.,* 2018). The transmission channels consist of exposure to contaminated mediums and inhalation of dust particles (Limmathurotsakul *et al.,* 2013). Clinically, the disease manifestation varies widely, from inconspicuous infections to severe or even fatal complications involving respiratory and other systems (Iowa State University, 2016).

In Thailand, particularly the Northeast region, melioidosis is endemic (Hinjoy *et al.,* 2018). The disease's history dates back to its first recorded case in 1955. Official data from "Report 506" reveals that between 2010 - 2019, there were annually an average of 3,115 cases (Bureau of Epidemiology, 2019). A model study estimated that 2,800 patients died in Thailand because of melioidosis (Hinjoy *et al.,* 2018). The financial implications are substantial, impacting both individual households and the national economy. Specific provinces in Thailand, such as Sa Kaeo and Nakhon Phanom, have documented significant economic burdens due to melioidosis (Chierakul *et al.,* 2013).

With technological advancements, remote-sensing data offers real-time insights into various environmental metrics, including normalized difference drought Index (NDDI), normalized difference vegetation index (NDVI), normalized difference water index (NDWI) and land surface temperature (LST). This availability of open geospatial data, combined with the surge in open-source geographic information system software, provides a potent tool for spatial epidemiological analysis (Chen *et al.,* 2012; Oliver *et al.,* 2005).

There has been no satellite-based environmental factors' study on melioidosis which limited the application of research results for appropriate measures to prevent the disease. Therefore, this study has two main objectives. First, it introduces the new data sources, which are the timely satellite-based indicators publicly accessible through Google Earth Engine. Second, it has applied the spatial statistical and regression analyses to the data set combining the official statistics and satellite data.

The main contribution of this study is twofold. First, it empirically confirmed the statistically significant associations between geospatial and socioeconomic conditions and the incidence rate of melioidosis. Second, technological resources and analytical frameworks introduced in this study offer a methodology that could inspire parallel investigations in other nations, potentially influencing future policy decisions.

2. Methodology

2.1 Study Design and Location

Thailand is a country in Southeast Asia spanning 513,120 km^2. In 2020, its population was 66,186,727 people (Bureau of Epidemiology, 2019). The geographical coordinates are latitudes 20°28'N and 5°36'S and longitudes 105°38'E and 97°22'W. It borders Myanmar and Laos in the North, Laos and Cambodia in the East, Malaysia in the South and the Andaman Sea and Myanmar in the West. Thailand is a country with mountains, hills, plains and coastlines stretching across the Gulf of Thailand (1,875 km) and Andaman Sea (740 km). The country has 4 regions: the Central, North, Northeast, and South. The geography of Central region consists of a large plain, a natural self-contained basin, and the clay-soil rice fields. The North is geographically characterized by high mountain area and steep river valleys. The Northeast, the largest region of Thailand, comprises a vast tableland bounded by mountain ranges and a substantial portion of the sandy- soil agricultural land. The Southern is mainly the peninsula with a combination of tidal flats and mangrove forests. Thailand has three seasons: rainy season between mid-May to mid-October, winter season between mid-October to mid-February and summer between mid-February to mid–May.

2.2 Population, Source of Information, and Study Variables

The study used secondary data on melioidosis registered in the National Notifiable Disease Surveillance System (Report 506), administrated by the Department of Disease Control, Ministry of Public Health of Thailand, from 2006 to 2020. These data were made available online at the Website by the Department of Disease Control, Ministry of Public Health of Thailand. A total of 37,870 cases were included. The criterion of being infected was the clinically diagnosed infection of Gram-negative bacillus *Burkholderia pseudomallei*. The diagnosis codes used for the infection were A24.1 – 24.4 of the International Statistical Classification of Diseases and Related Health Problem, 10th Revision (ICD - 10).

The satellite-based environmental factors included NDDI, NDVI, NDWI, daytime and night-time LST, urban and built-up area, cropland, and precipitation. All variables were obtained from Google Earth Engine. Data on NDDI, NDVI and NDWI were specifically obtained from the Moderate Resolution Imaging Spectroradiometer (MODIS) satellite (MOD13Q1) with a spatial resolution of 250 metres, and those on the urban and built-up area and cropland data were acquired from MODIS satellite (MOD12Q1 and MOD12C1) with a spatial resolution of 500 metres (Sulla-Menashe *et al.,* 2018).

Data on monthly precipitation averages were obtained from the integration of the global Cold Cloud Duration (CCD) rainfall estimate and Multi-Satellite Precipitation Analysis (TMPA 3B43) dataset collated by NASA and Japan's National Space Development Agency. Monthly accumulated precipitation data were available in spatial resolution of 0.25°, covering 0.50°N to 0.50°S from January 2003 to December 2019 (TRMM, 2022). The monthly accumulated precipitation data from January 2020 to December 2020 were provided by the Global Precipitation Climatology Centre (GPCC, 2022).

Data on daytime and night-time LST from MODIS were used as a time series of ground-level temperatures. Specifically, the time series of daytime LST was obtained from the MOD11A1 version 6, and that of night-time LST was generated by the MOD11A2 version 6 (Wan, 2019).

All satellite-based indicators were transformed to the monthly averages of each province which are compatible with the spatiotemporal resolution of melioidosis incidence.

2.3 Data Analysis

2.3.1 Spatial association

Spatial statistical analysis (i.e., global Moran's *I* and LISA (Local Indicator of Spatial Association) was employed to identify the spatial cluster of melioidosis incidence using QGIS (version 3.10.4) and GeoDa (version 1.14.0) (Anselin *et al.,* 2006; Steiniger *et al.,* 2013).

Moran's *I* is a statistical test for verifying spatial autocorrelation. Specifically, the obtained correlation coefficient quantitatively shows the relationship between the incidence of melioidosis and its surrounding values. Moran's *I* value ranges between −1 and 1. A value close to *I* indicates a highly positive spatial autocorrelation, and a value close to −1 indicates an extremely negative one. The zero value of Moran's *I* identifies no spatial autocorrelation.

Moran's *I* statistics is mathematically defined as:

$$I = \frac{[\sum_i \sum_j w_{ij}(x_i - \bar{x})(x_j - \bar{x})]}{\sum_i \sum_j w_{ij} \sum_i (x_i - x_j)/N}, \qquad (1)$$

where x_i is the variable of interest (melioidosis incidence, satellite-based indicators, etc.), N is the number of provinces and w_{ij} is the weight matrix.

In this study, Moran's *I* was used to examine the nationwide spatial autocorrelation. Furthermore, LISA method was applied to identify the clustering pattern's location. LISA is mathematically defined as:

$$I_i = \frac{N(x_i - \bar{x})[\sum_j w_{ij}(x_j - \bar{x})]}{\sum_i (x_i - \bar{x})^2}, \qquad (2)$$

where $i \neq j$, I_i is the LISA statistics of province i, and $I = \sum_i \frac{I_i}{N}$.

The outcome generated by LISA includes the cluster map showing four categories of spatial correlations, high–high, low–low, low–high and high–low (Anselin, 2003). The cases of high–high and low–low indicate the spatial cluster of positive correlation, and the areas of low–high and high–low define the spatial relationship of localized negative correlation.

2.3.2 Panel regression analysis

Multivariable analysis was applied to the panel dataset of melioidosis incidence and environmental factors for further investigation. Specifically, fixed-effect model (FEM) and random-effect model (REM) were estimated using Stata programme. In this study, the p-value less than 0.10 was considered statistically significant (Krikwood *et al.,* 2003; Stabel, 2021).

FEM is mathematically defined as:

$$lnY_{it} = \beta_1 lnNDDI_{it} + \beta_2 lnNDVI_{it} + \beta_3 lnNDWI_{it} + \beta_4 \ln daytimeLST_{it} + \beta_5 \ln nighttimeLST_{it} + \beta_6 lnUrban_{it} + \beta_7 \ln Cropland_{it} + \beta_k lnPrecipitation_{it} + \alpha_i + \varepsilon_{it} \quad (3)$$

where Y_{it} is the incidence rate of melioidosis in province i (76 provinces), and t = time (from 2006 to 2020)

$X_{k,it}$ is the satellite-based indicators of province i, and t = time

α_i is the unknown intercept for each entity

β_k is the coefficient for each satellite-based indicator

ε_{it} is the error term.

The empirical verification was alternatively undertaken on the basis of REM specification, which was mathematically denoted as:

$$lnY_{it} = \beta_1 lnNDDI_{it} + \beta_2 lnNDVI_{it} + \beta_3 lnNDWI_{it} + \beta_4 \ln daytimeLST_{it} + \beta_5 \ln nighttimeLST_{it} + \beta_6 lnUrban_{it} + \beta_7 \ln Cropland_{it} + \beta_k lnPrecipitation_{it} + \alpha + u_i + \varepsilon_{it} \quad (4)$$

where u_i is the individual residual which is the random characteristic of province i

α is the common intercept term and the others are identical to the specification of FEM.

It is also noted that u_i and ε_{it} are mutually independent. To select between FEM and REM, the Hausman test was applied. The mathematical specification of Hausman statistic is defined as:

$$H = \left(\hat{\beta}^{RE} - \hat{\beta}^{FE}\right)' \left[Var\left(\hat{\beta}^{RE}\right) - Var\left(\hat{\beta}^{FE}\right)\right]^{-1} \left(\hat{\beta}^{RE} - \hat{\beta}^{FE}\right) \quad (5)$$

where $\hat{\beta}^{RE}$ and $\hat{\beta}^{FE}$ are the vectors of estimated coefficients obtained from REM and FEM, respectively. Under the null hypothesis, the value of H has the $\chi 2$ (k) distribution. The test is undertaken by comparing with the critical value of $\chi 2$ (with k degrees of freedom) (Hausman, 1978).

3. Results and discussion

3.1 Distribution of melioidosis incidence from 2006 to 2020

An analysis of the region-level distribution of melioidosis incidence in Thailand showed that the region with the highest incidence rate was the Northeast, followed by the North. The 15-year trend endemic of the disease was similar. The provinces with the highest incidence of melioidosis were in the Northeast, which were Amnat Charoen, Mukdahan, Sisaket, Roi Et and Ubon Ratchathani as shown in Figure 1.

3.2 Local indicators of spatial association analysis

In addition to univariate spatial correlation, the spatial bivariate relationship was statistically verified by bivariate LISA. The correlation between satellite-based environmental factors and melioidosis incidence was analyzed, and the results are exhibited in Table 1 and Figures 2.

3.3 Panel regression model

Table 2 shows the results obtained from panel regression models for multivariable investigation. REM indicated that NDDI, NDVI, NDWI, daytime and night-time LST of the day, urban and built-up area, cropland, and precipitation were statistically associated with melioidosis incidence (p-value < 0.001). Similarly, FEM identified that all the variables were statistically associated with melioidosis incidence (p-value < 0.001), except for precipitation (p-value = 0.096). The estimated REM and FEM explained approximately 17.43% and 14.96% of melioidosis incidence, respectively. In addition, the Hausman test was conducted, identifying that FEM was preferred to REM.

Spatial analysis statistically quantified the degree of melioidosis infection in Thailand. The highest melioidosis incidence rate was found in the Northeast region (Hantrakun *et al.,* 2018). *B. pseudomallei* had a patchy spread in a rice crop (Wuthiekanun *et al.,* 2009). The outcomes of bivariate LISA using a 15-year dataset showed the localized positive correlation between satellite-based indicators (NDDI, NDVI, NDWI and cropland) and high melioidosis incidence rate. Similar to the main findings of Chakravorty *et al.* (2019), and Hantrakun *et al.* (2019), the present work indicated that the provinces with hotspot clusters were primarily the Northeast region because their physical conditions and climate are agricultural land and drought. In particular, the melioidosis incidence is influenced by environmental factors, such as the rainfall, vegetation, soil type, humidity, temperature and climatic variations, that favor the growth of the causative organism (Hempenstall *et al.,* 2019; Liu *et al.,* 2015; Birnie *et al.,* 2022). On the contrary, with its sprawling urban areas around Bangkok and expanding industrial estates in many provinces, the central region was the main location for most coldspot clusters, indicating its low incidence rate of melioidosis induced by those factors (Hinjoy *et al.,* 2018). Most of the population at risk of contracting melioidosis lives in rural areas, particularly those who are exposed to soil and water containing melioidosis from performing occupation, ingestion, and inhalation, such as plantation workers. In addition, social impacts of lifestyle changes are reflected in seasonal movement and increasing urbanization (Sia *et al.,* 2021; Limmathurotsakul *et al.,* 2013).

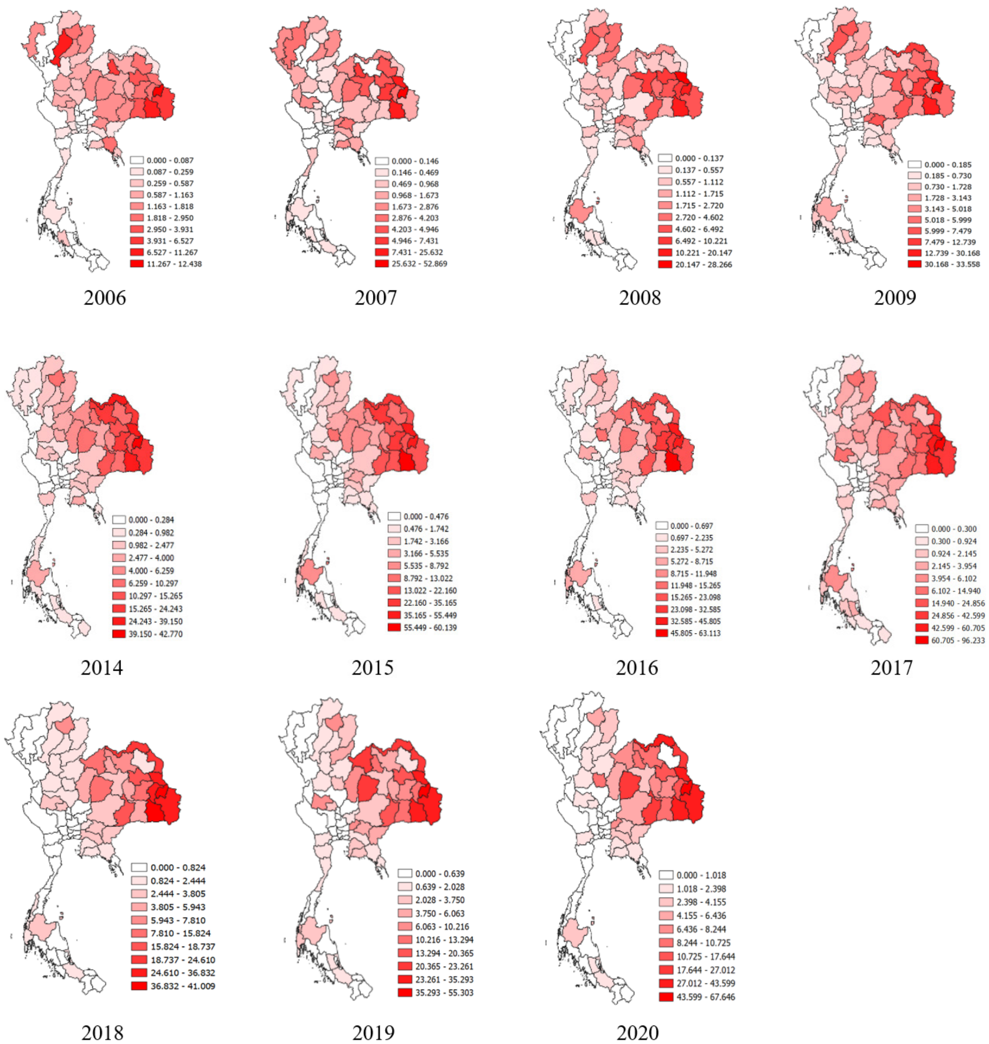

Figure 1. Distribution of melioidosis incidence in 2006 – 2020

Table 1. Bivariate Moran's I statistics of melioidosis incidence and satellite-based environmental factors (2006 – 2020)

Year	LISA (Moran's *I*) (variable)							
	NDDI	NDVI	NDWI	LST day	LST night	Urban	Cropland	Precipitation
2006	0.665	-0.282	-0.569	0.274	-0.179	0.136	0.455	-0.162
2007	0.603	-0.346	-0.550	0.253	-0.029	0.041	0.381	-0.192
2008	0.588	-0.356	-0.559	0.223	-0.065	0.074	0.398	-0.184
2009	0.656	-0.337	-0.576	0.257	-0.105	0.084	0.431	-0.238
2010	0.684	-0.368	-0.606	0.360	-0.056	0.083	0.476	-0.347
2011	0.682	-0.330	-0.627	0.277	-0.248	0.067	0.462	-0.152
2012	0.673	-0.285	-0.593	0.184	-0.127	0.024	0.462	-0.342
2013	0.710	-0.366	-0.609	0.304	-0.162	0.040	0.487	-0.145
2014	0.666	-0.299	-0.534	0.135	-0.215	0.019	0.496	-0.062
2015	0.660	-0.334	-0.538	0.237	-0.143	0.009	0.469	-0.129
2016	0.524	-0.178	-0.389	0.108	-0.181	-0.006	0.419	-0.121
2017	0.555	-0.234	-0.426	0.147	-0.089	-0.023	0.422	-0.093
2018	0.882	-0.282	-0.555	0.288	-0.233	0.021	0.451	-0.074
2019	0.598	-0.294	-0.480	0.267	0.036	0.041	0.466	0.095
2020	0.541	-0.251	-0.424	0.206	0.065	0.051	0.470	-0.173

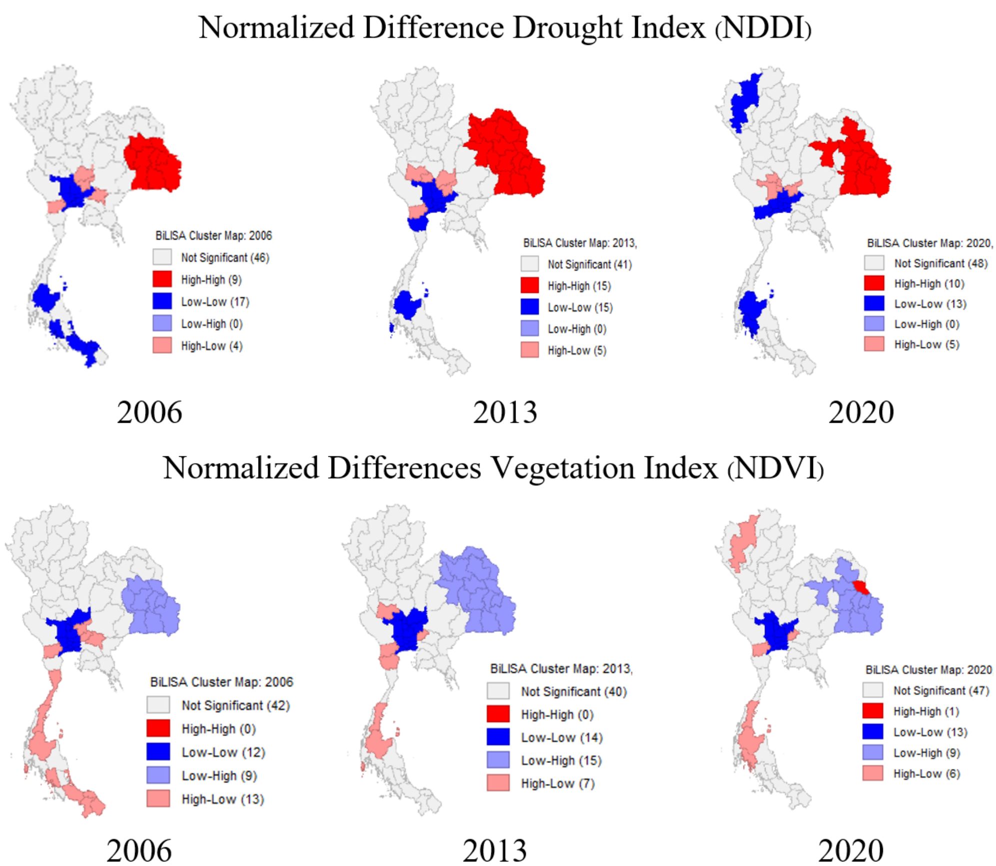

Figure 2. Cluster maps of LISA: Localized associations between NDDI, NDVI, NDWI, daytime LST, night-time LST, urban and built-up area, cropland, precipitation, and melioidosis incidence for 2006, 2013, 2020.

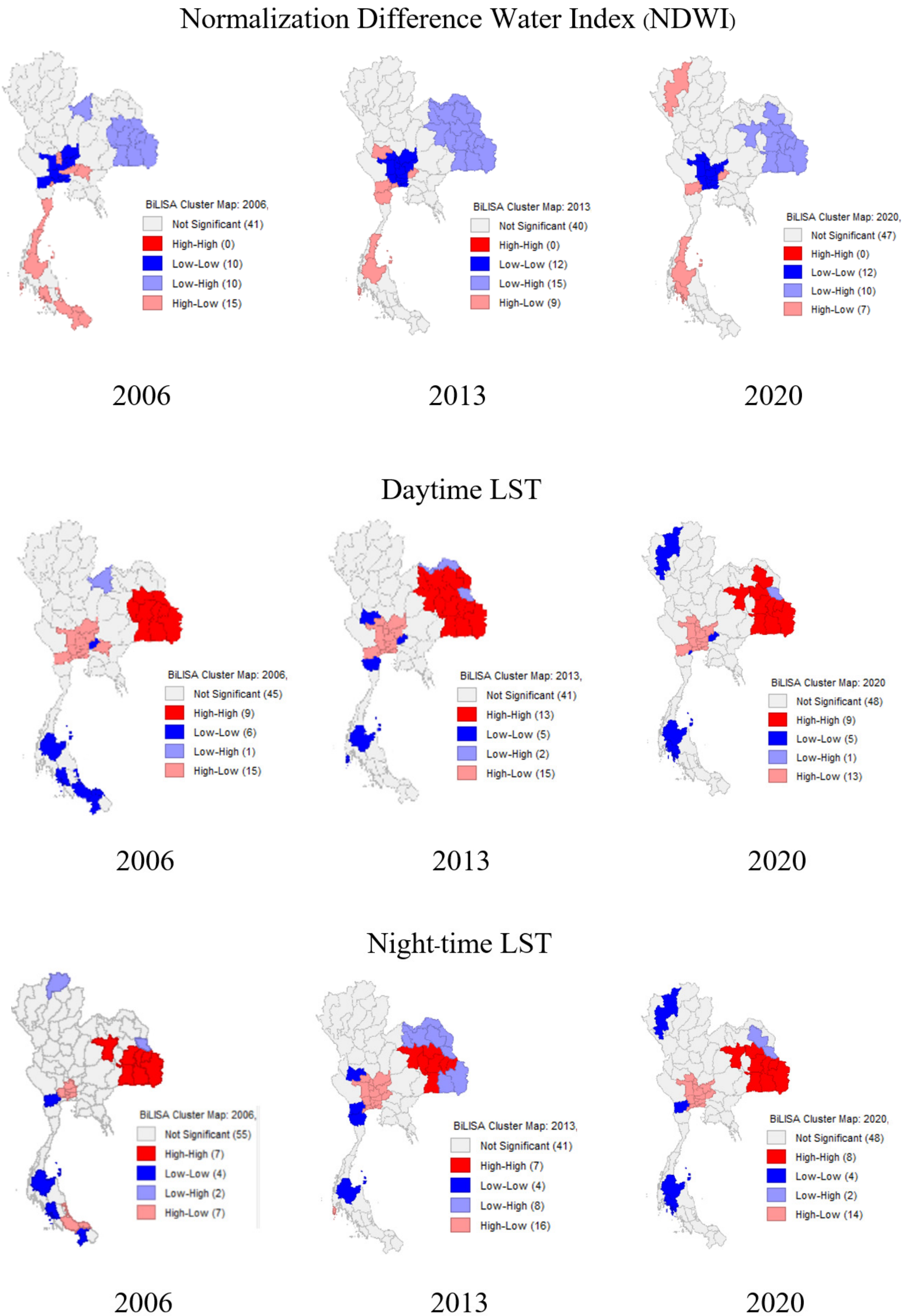

Figure 2 (Cont.) Cluster maps of LISA: Localized associations between NDDI, NDVI, NDWI, daytime LST, night-time LST, urban and built-up area, cropland, precipitation, and melioidosis incidence for 2006, 2013, 2020.

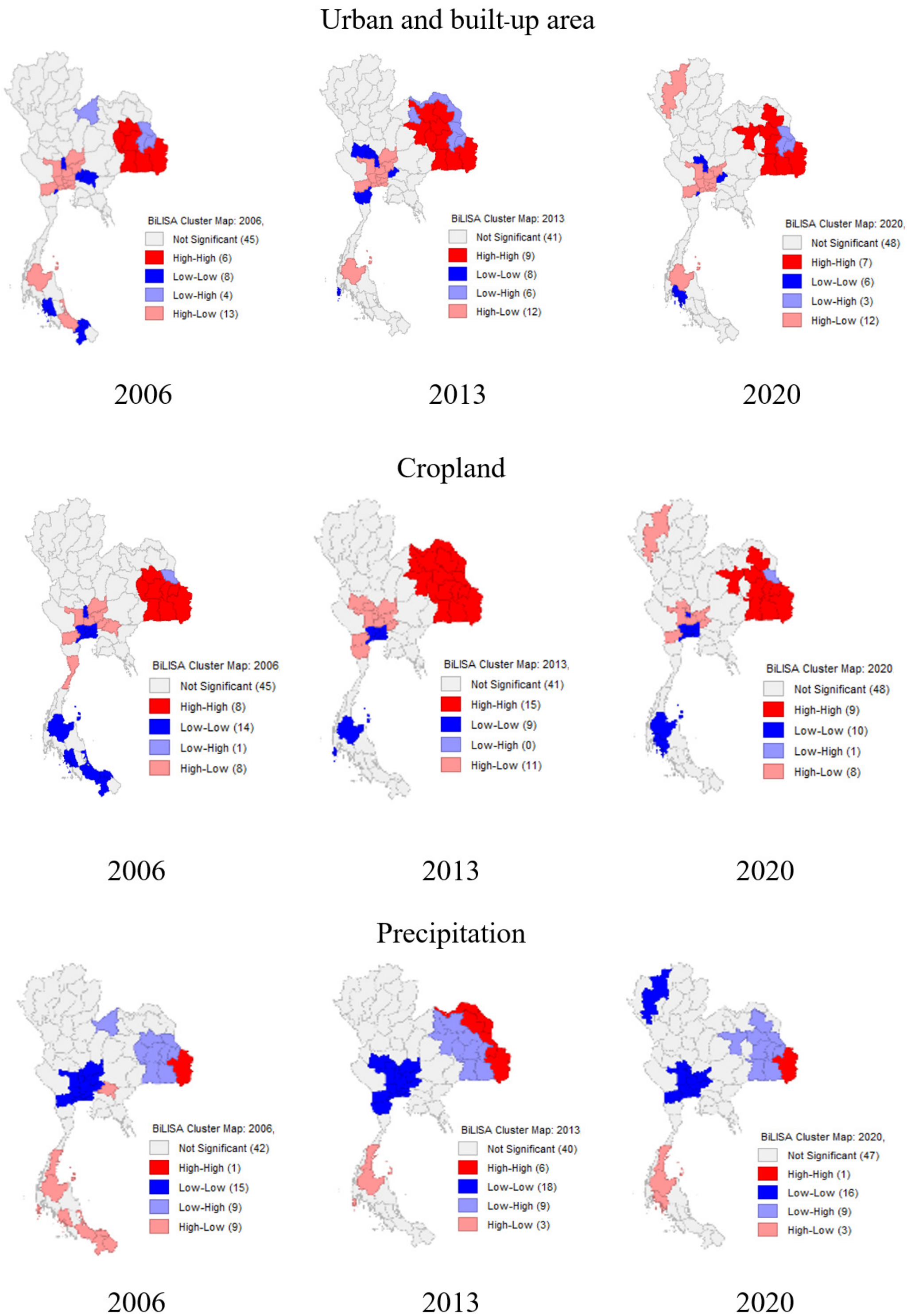

Figure 2 (Cont.) Cluster maps of LISA: Localized associations between NDDI, NDVI, NDWI, daytime LST, night-time LST, urban and built-up area, cropland, precipitation, and melioidosis incidence for 2006, 2013, 2020.

Table 2. Estimated parameters obtained from panel regression (REM and FEM)

Independent variable	Panel regression (random effect)	Panel regression (fixed effect)
Constant	4.547 ($p < 0.001$)	5.101 ($p < 0.001$)
ln NDDI	-1.108 ($p < 0.001$)	-0.755 ($p < 0.001$)
ln NDVI	1.400 ($p < 0.001$)	1.083 ($p < 0.001$)
ln NDWI	-3.550 ($p < 0.001$)	-3.382 ($p < 0.001$)
ln DaytimeLST	-1.230 ($p < 0.001$)	-1.300 ($p < 0.001$)
ln Night-timeLST	0.216 ($p < 0.001$)	0.188 ($p < 0.001$)
ln Urban	-0.081 ($p < 0.001$)	-0.082 ($p < 0.001$)
ln Cropland	0.044 ($p < 0.001$)	0.034 ($p < 0.001$)
ln Precipitation	0.034 ($p < 0.001$)	0.008 ($p = 0.096$)
F (8, 13492)		449.09
Prob > F		0.0000
R-squared	0.1743	0.1495
Wald $chi^2(8)$	3,216.55	
$P > chi^2$	0.0000	
No. of observations	13,680	13,680
Hausman Test:		
$Chi^2(8)$	347.18	
$Prob > chi^2$	0.0000	

The results obtained from panel regression analysis indicated that all satellite-based environmental indicators were statistically significant. Specifically, NDVI, night-time LST and cropland had a statistically significant positive association with melioidosis incidence. Meanwhile, NDDI, NDWI, daytime LST and urban and built-up area had a statistically significant negative relationship with melioidosis incidence.

As documented by Gu *et al.* (2007), NDDI, NDVI and NDWI are satellite-based indices of climate conditions. Given that environmental factors can influence the presence of the pathogen *B. pseudomallei,* variations of NDDI, NDVI and NDWI are statistically associated with the incidence of melioidosis. Specifically, the high value of NDDI represents the great severity of drought, and the rising magnitude of NDWI indicates the expansion of the water body. Both conditions are extreme environments for pathogen *B. pseudomallei* (Ribolzi *et al.,* 2016; Gassiep *et al.,* 2020). Thus, the regression coefficients of NDDI and NDWI were statistically negative.

NDVI and cropland are indicators jointly representing agricultural activity. Specifically, NDVI indicates crop density (i.e. concentration of leaf or chlorophyll), and cropland index implies the cultivation area. In Thailand, farmers in rural areas usually work barefoot in the farmland, especially in the rice field (Hinjoy *et al.,* 2018). Panel regression analysis showed that NDVI and cropland had a statistically significant positive association with melioidosis incidence. These results are analogous to previous literature stating that the infection is related to exposure to soil contaminated with *B. pseudomallei* (Kaestli *et al.,* 2016; Liu *et al.,* 2015; Paksanont *et al.,* 2018). In Myanmar, Swe *et al.* (2021) reported that the concentration of *B. pseudomallei* in pastureland is 19.46 times higher than that in residential areas. Some investigators have noted that the influence of soil and vegetation type on the growth of *B. pseudomallei* is less well defined (Hempenstall *et al.,* 2019). Some studies have found a higher proportion of silt and clay particles, and an alkaline (Goodrick *et al.,* 2018), provide conditions preferred by the bacteria, but other studies have found a positive association with the proportion of sand (Hantrakum *et al.,* 2016).

Temperature is an important factor for the growth and survival of *B. pseudomallei* which only thrives at 37 °C - 42 °C (Kaestli *et al.,* 2016; Limmathurotsakul *et al.,* 2013). The obtained coefficients of daytime and night-time LST were statistically negative and positive, respectively. These results correspond to the favourable temperature range for *B. pseudomallei*. On the one hand, the high daytime LST leads to an extreme environment above the maximum of the favourable range. On the other hand, the high night-time LST increases the temperature to a suitable degree for *B. pseudomallei* growth.

The regression coefficient of precipitation (i.e. rainfall) was positive and statistically significant for FEM and REM. This result is parallel to previous studies stating that rainfall in Darwin, Australia (Kaestli *et al.,* 2016; Currie *et al.,* 2004; Currie *et al.,* 2010), and storms such as typhoons in Taiwan (Chen *et al.,* 2015) is associated with melioidosis incidence, which is contacting soil, ingesting, or inhaling aerosolization of dry dust. On the contrary, other study was a negative association between the total annual rainfall and the number of melioidosis cases in each year in Thailand (Limmathurotsakul *et al.,* 2010.According to current literature, there is no correlation between yearly rainfall and an increase in the incidence of melioidosis. Understanding of how rainfall affects melioidosis will be improved by further research into the climate of the disease.

As documented by Hinjoy *et al.* (2018), Hantrakun et al. (2006) and Savelkoel *et al.* (2022), the underreported number of infected cases is a global concern, and melioidosis is widely recognised as a neglected tropical disease. The present study suggested the development of a monitoring system using satellite data to estimate the risk exposure and predict the likelihood of infected cases. This approach will provide timely information with low budget burden and can also be implemented in other developing countries with high melioidosis incidence.

This study has some limitations. Firstly, serious concerns have been raised regarding the underreported statistics of melioidosis incidence in Thailand. Some studies stated that melioidosis is often misdiagnosed due to the lack of expertise and supportive facility. Specifically, patients in rural provinces do not have access to microbiology laboratories. Furthermore, some cases may be misdiagnosed because the clinical symptoms are similar to other diseases, such as dengue fever, leptospirosis, influenza and tuberculosis. Hence, the obtained regression coefficients might not precisely present the actual relationship between environmental factors and melioidosis incidence. Secondly, additional variables should be included to extend the scope of the analysis, allowing a comprehensive investigation of influencing factors and risk exposures. Thirdly, new computational techniques, such as machine learning, should be applied. These new methods can potentially enhance the predictive power, enabling the precise forecast for future prevention policy.

4. Conclusion

Bivariate LISA results showed the statistically significant correlation between each satellite-based indicator and melioidosis incidence. Moreover, LISA geographically identified that the statistically significant clusters of localized associations were mainly located in the Northeast region. Panel regressions, FEM and REM, were applied to alternatively explore the multivariable relationships. The obtained regression coefficients of all variables were statistically significant, implying that specific environmental conditions and economic activity are related to melioidosis incidence. These key findings suggest the potential application of satellite-based data for the timely monitoring and prediction of melioidosis incidence. Relevant agencies and public health authorities could use the map to identify environmental risk factors of high-risk areas as well as develop more efficient preventive and control measures for melioidosis. In addition, they could effectively communicate and advocate for appropriate practices to people at risk to reduce environmental exposure to reduce their health risks.

Acknowledgement

The authors are grateful to the Department of Disease Control, Ministry of Public Health of Thailand, for providing the information in Report 506.

Reference

Anselin L. An introduction to spatial autocorrelation analysis with GeoDa [Internet]. IL: University of Illinois; 2003 [cited 2022 Apr 22]. Available form: https://personal.tdallas.edu/~briggs/poec6382/geoda_spauto.pdf

Anselin L, Syabri I, Kho Y. Geo Da. An Introduction to Spatial Data Analysis. In: Fischer M, Getis A, editors. Handbook of Applied Spatial Analysis. Berlin: Springer Berlin Heidelberg; 2009. p. 73-89.

Birnie E, Biemond JJ, Wiersinga WJ. Drivers of melioidosis endemicity: epidemiological transition, zoonosis, and climate change. Curr Opin Infect Dis [Internet]. 2022 [cited 2022 Apr 22]; 35(3): 196-204. Available form: https://www.ncbi.nlm.nih.gov/pmc/articles/PMC10128909/

Bureau of Epidemiology. Annual Epidemiology Surveillance Report 2019 [Internet]. 2020 [cited 2022 Apr 22]. Available form: https://ddc.moph.go.th/uploads/publish/1129820210620030431.pdf

Chakravorty A, Heath CH. Melioidosis: An updated review. Aust J Gen Pract. 2019; 48(5): 327-32. doi: 10.31128/AJGP-04-18-4558.

Chen H, Yan M, Yang X, Chen Z, Wang G, Schmidt-Vogt D, et al. Spatial distribution and temporal variation of high fluoride contents in groundwater and prevalence of fluorosis in humans in Yuanmou County, Southwest China. J Hazard Mater. 2012 Oct 15; 235-236: 201-9. doi: 10.1016/j.jhazmat.2012.07.042.

Chen PS, Chen YS, Lin HH, Liu PJ, Ni WF, Hsueh PT, et al. Airborne Transmission of Melioidosis to Humans from Environmental Aerosols Contaminated with B. pseudomallei. PLoS Negl Trop Dis. 2015; 9(6): e0003834. PMID: 26061639.

Bhengsri S, Lertiendumrong J, Baggett HC, Thamthitiwat S, Chierakul W, Tisayaticom K, et al. Economic Burden of Bacteremic Melioidosis in Eastern and Northeastern, Thailand. Am J Trop Med Hyg. 2013; 89(2): 369–73. doi: 10.4269/ajtmh.13-0148.

Chowdhury S, Barai L, Afroze SR, Ghosh PK, Afroz F, Rahman H, et al. The epidemiology of Melioidosis and its association with Diabetes Mellitus: A systematic review and meta-analysis. Pathogens. 2022; 11(2): 149. doi: 10.3390/pathogens11020149

Currie BJ, Jacups SP, Cheng AC, Fisher DA, Anstey NM, Huffam SE, et al. Melioidosis epidemiology and risk factors from a prospective whole-population study in northern Australia. Trop Med Int Health. 2004; 9(11): 1167-74. doi: 10.1111/j.1365-3156.2004.01328.x..

Currie BJ, Ward L, Cheng, AC. The epidemiology and clinical spectrum of Melioidosis: 540 cases from the 20 year Darwin prospective study. PLoS Negl Trop Dis. 2010; 4(11): e900. PMID: 21152057

Gassiep I, Armstrong M, Norton R. Human Melioidosis. Clin Microbiol Rev. 2020; 33(2): e00006-19. doi: 10.1128/CMR.00006-19.

Goodrick I, Todd G, Stewart J. Soil characteristics influencing the spatial distribution of melioidosis in Far North Queensland, Australia. Epidemiol Infect. 2018; 146(12): 1602-7. doi: 10.1017/S0950268818001188.

Global Precipitation Climatology Centre (GPCC). GOCC Full Data Monthly Product Version 2020 [Internet]. 2022 [cited 2022 May 22]. Available form: https://opendata.dwd.de/climate_environment/GPCC/html/fulldata-monthly_v2020_doi_ download.html

Gu Y, Brown JF, Verdin JP, Wardlow B. A five-year analysis of MODIS NDVI and NDWI for grassland drought assessment over the central Great Plains of the United States. Geophys Res Lett. 2007; 34(6). doi: 10.1029/2006GL029127.

Hantrakun V, Rongkard P, Oyuchua M, Amornchai P, Lim C, Wuthiekanun V, et al. Soil Nutrient Depletion Is Associated with the Presence of *Burkholderia pseudomallei*. Appl Environ Microbiol. 2016; 82(24): 7086-92. doi: 10.1128/AEM.02538-16.

Hantrakun V, Thaipadungpanit J, Rongkard P, Srilohasin P, Amornchai P, Langla S, et al. Presence of B. thailandensis and B. thailandensis expressing B. pseudomallei-like capsular polysaccharide in Thailand, and their associations with serological response to B. pseudomallei. Borlee BR, editor. PLoS Negl Trop Dis. 2018; 12(1): e0006193.

Hantrakun V, Kongyu S, Klaytong P, Rongsumlee S, Day NPJ, Peacock SJ, et al. Clinical Epidemiology of 7126 Melioidosis Patients in Thailand and the Implications for a National Notifiable Diseases Surveillance System. Open Forum Infect Dis. 2019; 6(12): ofz498. doi: 10.1093/ofid/ofz498.

Hausman JA. Specification Tests in Econometrics. Econometrica. 1978; 46(6): 1251–71. doi: 10.2307/1913827

Hempenstall AJ, Smith S, Stanton D, Hanson J. Melioidosis in the Torres Strait Islands, Australia: Exquisite Interplay between Pathogen, Host, and Environment. Am J Trop Med Hyg. 2019; 100(3): 517-21. doi: 10.4269/ajtmh.18-0806.

Hinjoy S, Hantrakun V, Kongyu S, Kaewrakmuk J, Wangrangsimakul T, Jitsuronk S, et al. Melioidosis in Thailand: Present and Future. Trop Med Infect Dis. 2018; 3(2): 38. doi: 10.3390/tropicalmed3020038.

Iowa State University. Melioidosis: Pseudoglander, whitmore disease [Internet]. 2016 [cited 2022 Apr 22]. Available from: https://www.cfsph.iastate.edu/Factsheets/pdfs/melioidosis.pdf

Kaestli M, Grist EPM, Ward L, Hill A, Mayo M, Currie BJ. The association of melioidosis with climatic factors in Darwin, Australia: A 23-year time-series analysis. J Infect. 2016; 72(6): 687–97. doi: 10.1016/j.jinf.2016.02.015.

Krikwood BR, Sterne JAC. Essential Medical Statistics. 2nd ed. Malden, MA: Blackwell Publishing; 2003.

Limmathurotsakul D, Wongratanacheewin S, Teerawattanasook N, Wongsuvan G, Chaisuksant S, Chetchotisakd P, et al. Increasing incidence of human melioidosis in Northeast Thailand. Am J Trop Med Hyg. 2010; 82(6): 1113-7. doi: 10.4269/ajtmh.2010.10-0038.

Limmathurotsakul D, Kanoksil M, Wuthiekanun V, Kitphati R, deStavola B, Day NP, et al. Activities of daily living associated with acquisition of melioidosis in northeast Thailand: a matched case-control study. PLoS Negl Trop Dis. 2013; 7(2): e2072. doi: 10.1371/journal.pntd.0002072.

Liu X, Pang L, Sim SH, Goh KT, Ravikumar S, Win MS, et al. Association of Melioidosis incidence with rainfall and humidity, Singapore, 2003–2012. Emerg Infect Dis. 2015; 21(1): 159–62. doi: 10.3201/eid2101.140042.

Mukhopadhyay C, Shaw T, Varghese GM, Dance DAB. Melioidosis in South Asia (India, Nepal, Pakistan, Bhutan and Afghanistan). Trop Med Infect Dis. 2018; 3(2): 51. doi: 10.3390/tropicalmed3020051.

Oliver MN, Smith E, Siadaty M, Hauck FR, Pickle LW. Spatial analysis of prostate cancer incidence and race in Virginia, 1990-1999. Am J Prev Med. 2006 Feb;30(2 Suppl):S67-76. doi: 10.1016/j.amepre.2005.09.008.

Paksanont S, Sintiprungrat K, Yimthin T, Pumirat P, Peacock SJ, Chantratita N. Effect of temperature on *Burkholderia pseudomallei* growth, proteomic changes, motility and resistance to stress environments. Sci Rep. 2018; 8(1): 9167. doi: 10.1038/s41598-018-27356-7.

Ribolzi O, Rochelle-Newall E, Dittrich S, Auda Y, Newton PN, Rattanavong S, et al. Land use and soil type determine the presence of the pathogen *Burkholderia pseudomallei* in tropical rivers. Environ Sci Pollut Res. 2016; 23(8): 7828–39. doi: 10.1007/s11356-015-5943-z.

Rolim DB, Vilar DC, Sousa AQ, Miralles IS, Almeida de Oliveira C, Harnett G, et al. Melioidosis, Northeastern Brazil. Emerg Infect Dis. 2005, 11(9): 1458–60. doi: 10.3201/eid1109.050493

Savelkoel J, Dance DAB, Currie BJ, Limmathurotsakul D, Wiersinga WJ. A call to action: time to recognise melioidosis as a neglected tropical disease. Lancet Infect Dis. 2022; 22(6): e176-82. doi: 10.1016/S1473-3099(21)00394-7.

Sia TLL, Mohan A, Ooi MH, Chien SL, Tan LS, Goh C, et al. Epidemiological and Clinical Characteristics of Melioidosis Caused by Gentamicin-Susceptible *Burkholderia pseudomallei* in Sarawak, Malaysia. Open Forum Infect Dis. 2021; 8(10): ofab460.

Stahel WA. New relevance and significance measures to replace p-values. Plos One. 2021; 16(6): e0252991. doi: 10.1371/journal.pone.0252991

Steiniger S, Hunter A. The 2012 free and open source GIS software map – A Guide to facilitate research, development and adoption. Comput Environ Urban Syst 39[Internet]. 2013 [cited 2022 May 22]. Available from: https://doi.org/10.1016/j.compenvurbsys.2012.10.003

Steinmetz I, Wagner GE, Kanyala E, Sawadogo M, Soumeya H, Teferi M, et al. Melioidosis in Africa: Time to uncover the true disease load. Trop Med Infect Dis. 2018; 3(2): 62. doi: 10.3390/tropicalmed3020062

Sujuritphong P, Suggaravetsiri P, Vaeteewootachan K. Factors association with patients suffering from Melioidosis at the Khok Sri Suphan Hospital, Sakonnakhon Province. KKU Journal for Public Health Research. 2014; 7(1): 80-6.

Sulla-Menashe D, Friedl MA. User Guide to Collection 6 MODIS Land Cover (MCD12Q1 and MCD12C1) Product [Internet]. 2018 [cited 2022 Apr 22]. Available from: https://lpdaac.usgs.gov/documents/101/MCD12_User_Guide_V6.pdf

Swe MMM, Win MM, Cohen J, Phyo AP, Lin HN, Soe K, et al. Geographical distribution of *Burkholderia pseudomallei* in soil in Myanmar. PLOS Negl Trop Dis. 2021; 15(5): e0009372. doi: 10.1371/journal.pntd.0009372

Tropical Rainfall Measuring Mission (TRMM). Climate data [Internet]. 2022 [cited 2022 May 22]. Available form: https://climatedataguide.ucar.edu/climate-data/trmm-tropical-rainfall-measuring-mission

Wan Z. Collection-6 MODIS land surface temperature products users' guide. ERI, University of California, Santa Barbara [Internet]. 2019 [cited 2022 May 22]. Available from: https://landweb.modaps.eosdis.nasa.gov/QA_WWW/forPage/user_guide/061/MOD11_C61_UsersGuide_revSudipta_revPete_Final.pdf

White NJ. Melioidosis. Lancet. 2003; 361(9370): 1715–22. doi: 10.1016/s0140-6736(03)13374-0.

Wuthiekanun V, Smith MD, Dance DA, White NJ. Isolation of Pseudomonas pseudomallei from soil in north-eastern Thailand. Trans R Soc Trop Med Hyg. 1995; 89(1): 41–3. doi: 10.1016/0035-9203(95)90651-7.

Wuthiekanun V, Limmathurotsakul D, Chantratita N, Feil EJ, Day NPJ, Peacock SJ. *Burkholderia pseudomallei* Is Genetically Diverse in Agricultural Land in Northeast Thailand. PLoS Negl Trop Dis. 2009; 3(8): e496. doi: 10.1371/journal.pntd.0000496.